Upper Critical Field Peculiarities of Superconducting YNi_2B_2C and $LuNi_2B_2C$

S. V. Shulga,* S.-L. Drechsler, G. Fuchs, and K.-H. Müller
Institut für Festkörper- und Werkstofforschung Dresden e.V., Postfach 270016, D-01171 Dresden, Germany

K. Winzer, M. Heinecke, and K. Krug
1. Physikalisches Institut, Universität Göttingen, Bunsenstrasse 9, D-37073 Göttingen, Germany
(Received 7 October 1997)

We present new upper critical field $H_{c2}(T)$ data in a broad temperature region $0.3\ \mathrm{K} \le T \le T_c$ for $LuNi_2B_2C$ and YNi_2B_2C single crystals with well characterized low impurity scattering rates. The absolute values for all T, in particular, $H_{c2}(0)$, and the sizable positive curvature (PC) of $H_{c2}(T)$ at high and intermediate T are explained quantitatively within an effective two-band model. The failure of the isotropic single-band approach is discussed in detail. Supported by de Haas–van Alphen data, the superconductivity reveals direct insight into details of the electronic structure. The observed maximal PC near T_c gives strong evidence for clean limit type-II superconductors. [S0031-9007(98)05338-1]

PACS numbers: 74.60.Ec, 74.20.–z, 74.70.Ad

The discovery [1,2] of superconductivity in transition metal borocarbides has generated large interest due to their relatively high transition temperatures $T_c \sim 15$ to 23 K and due to the relation between the mechanisms of superconductivity in these compounds, in cuprates, and in ordinary transition metals. Another highlight is the coexistence of magnetism and superconductivity in some of these compounds containing rare earth elements [3–5]. A study of the nonmagnetic compounds, such as LNi_2B_2C, with $L = \mathrm{Lu, Y, Th, Sc}$ [6], is a prerequisite for the understanding of their magnetic counterparts. Experimental data for $LuNi_2B_2C$ [7] demonstrate, besides a maximal positive curvature (PC) of $H_{c2}(T)$ near T_c, observed also for YNi_2B_2C [4,8,9], a weak T-dependent anisotropy within the tetragonal basal plane and a T-independent out-of-plane anisotropy of the upper critical field H_{c2}. Both anisotropies have been described [7] in terms of nonlocal corrections to the Ginzburg-Landau (GL) equations. In this picture the PC of H_{c2}^c ($\vec{H} \parallel$ to the tetragonal c axis) is caused, almost entirely, by the basal plane anisotropy. However, it should be noted that the reported anisotropy of H_{c2} for YNi_2B_2C is significantly smaller than for $LuNi_2B_2C$ [7,9,10], whereas its PC is comparable or even larger. Further explanations of the unusual PC of $H_{c2}(T)$, such as quasi-2D fluctuations [11], are excluded by the underestimation of $H_{c2}(T)$ at low T [9] and the observed weak anisotropy. The quantum critical point scenario [12], as well as the bipolaronic scenario [13], can be disregarded because the slope of $H_{c2}(T)$ decreases for $T \to 0$ (see Fig. 1). Local density approximation (LDA) band structure calculations [14,15] predict a nearly isotropic electronic structure with rather complicated bands near the Fermi level E_F. However, in analyzing the superconductivity in terms of an isotropic *single*-band (ISB) Eliashberg model, the multiband character and the anisotropic Fermi surface have been widely ignored so far.

Here we present and analyze theoretically the new data of $H_{c2}(T)$ in a broad interval $0.3\ \mathrm{K} \le T \le T_c$ for high purity $LuNi_2B_2C$ and YNi_2B_2C single crystals. We show that typical features of both compounds, such as $H_{c2}(0) \sim 8$–10 T and the unusual PC of $H_{c2}(T)$ for $T \gtrsim 0.5T_c$, cannot in any way be explained consistently with the normal state properties within the ISB approach. Instead we propose a two-band model (TBM) approach. To clarify its relationship to the extended saddle-point model [16], which also predicts a PC, is beyond the scope of this Letter.

Platelet shaped $LuNi_2B_2C$ and YNi_2B_2C single crystals with a mass of $\sim$1 mg were grown by a high-temperature flux technique with Ni_2B as flux. The values of T_c, 16.5 K, and 15.7 K, have been determined by low-field ac susceptibility $\chi(T)$ with transition widths $\Delta T_c = 0.2$ K. The upper critical field $H_{c2}^c(T)$ along the c axis, shown in Figs. 1 and 2, has been measured resistively for fixed T adopting the midpoint criterion, $\rho(H_{c2}, T) = 0.5\rho(H = 0, T = 17\ \mathrm{K}) \equiv 0.5\rho_n$. The transition width $\Delta H = [H(\rho = 0.9\rho_n) - H(\rho = 0.1\rho_n)]$ increases up to 0.75 T (1.5 T for $LuNi_2B_2C$) at $T < 0.5$ K starting from a nearly constant value of 0.3 T at $T > 4$ K (8 K for $LuNi_2B_2C$). The low residual resistivity $\rho(0) \approx \rho_n = 2.5\ \mu\Omega$ cm and the ratio $\rho(300\ \mathrm{K})/\rho_n = 43$ (27 for $LuNi_2B_2C$), together with the observations of magnetoquantum oscillations [17–19], indicate a high quality and a low impurity content of our samples. This suggests that we are in the clean limit in terms of the traditional theory of type-II superconductors [20]. In this limit, one has to consider the electronic structure in more detail. We restrict ourselves to an effective two-band model [21] which, especially on the simple Bardeen-Cooper-Schrieffer (BCS) level, has a long history [22]. Because of the neglect of strong coupling effects, a BCS-like theory is not expected to describe real superconductors quantitatively. Such effects must be studied within the Eliashberg theory [23–27]. To calculate H_{c2}, we have solved numerically the corresponding linearized equations of Ref. [23],

 0031-9007/98/80(8)/1730(4)$15.00

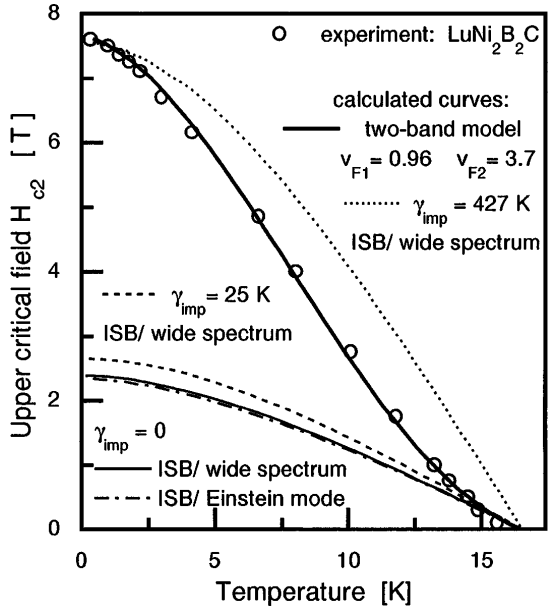

FIG. 1. Experimental data for $H_{c2}(T)$ of $LuNi_2B_2C$ (magnetic field $\vec{H}\|$ the c axis) compared with theoretical curves: (i) the isotropic single band model with Fermi velocity $v_F = 2.76 \times 10^7$ cm/s and various impurity scattering rates $\gamma_{\rm imp}$; (ii) the two-band model with v_{Fi} $(i = 1, 2)$ in units of 10^7 cm/s.

$$\tilde{\omega}_i(n) = \omega_n + \pi T \sum_{j,m} [\lambda_{i,j}(m - n) + \delta_{mn}(\gamma_{{\rm imp};i,j} + \gamma^s_{{\rm imp};i,j})/2\pi T] \, {\rm sgn}(\omega_m) , \quad (1)$$

$$\tilde{\Delta}_i(n) = \pi T \sum_{j,m} [\lambda_{i,j}(m - n) - \mu^* \delta_{ij} \theta(\omega_c - |\omega_m|) + \delta_{mn}(\gamma_{{\rm imp};i,j} - \gamma^s_{{\rm imp};i,j})/2\pi T] \times \chi_j(m) \tilde{\Delta}_j(m) , \quad (2)$$

$$\chi(n) = (2/\sqrt{\beta_i}) \int_0^\infty dq \exp(-q^2) \times \tan^{-1}\{q\sqrt{\beta_i}/[|\tilde{\omega}_i(n)| + i\mu_B H_{c2} \, {\rm sgn}(\omega_n)]\} , \quad (3)$$

$$\beta_i = eH_{c2} v_{Fi}^2/2 , \quad (4)$$

$$\lambda_{i,j}(n) = \int_0^\infty d\omega \, \omega \alpha^2_{i,j} F(\omega)/(\omega^2 + \omega_n^2) . \quad (5)$$

The bands at E_F are labeled by i,j. Here $\omega_n = 2\pi T(2n + 1)$ are the Matsubara frequencies, $\alpha_i^2 F(\omega)$ and $\tilde{\Delta}_i$ denote the spectral density and the superconducting order parameter of the ith band, respectively. In our approach, as in any two-band model, two gaps, below and above the BCS value of $3.5 k_B T_c$, occur naturally. In general, interband coupling $(i \neq j)$ mediated by phonons $[\alpha^2_{i,j} F(\omega)]$ and impurities is important. Since there is no experimental evidence [28,29] for the presence of magnetic impurities in high quality samples, we neglect the magnetic scattering rate $\gamma^s_{\rm imp}$. For the quantification of the nonmagnetic counterpart $\gamma_{\rm imp} \approx 2\pi T_D$, the Dingle temperatures T_D, measured by the de Haas–van Alphen (dHvA) effect, are very suitable [17–19]. The experimental values $T_D = 2.8$ and 4 K reveal $\gamma_{\rm imp} = 18$ and 25 K for our YNi_2B_2C and $LuNi_2B_2C$ single crystals, respectively, indicating that the clean limit is reached since $\gamma_{\rm imp} \leq 2\Delta_0 \approx 51$ K holds for both samples, where $2\Delta_0$ denotes the smaller of the two gaps. Hence, the scattering by impurities can be neglected by setting $\gamma_{\rm imp} = 0$. In the weak coupling limit of an ISB case, Eqs. (1)–(5) are equivalent to the standard theory [30]. Any anisotropy of H_{c2} can be described by a similar, but much more tedious, system of equations [26]. Since the measured anisotropy is relatively weak, it will be ignored for the sake of simplicity. Therefore, only $H^c_{c2}(T)$'s will be compared with those of our isotropic models.

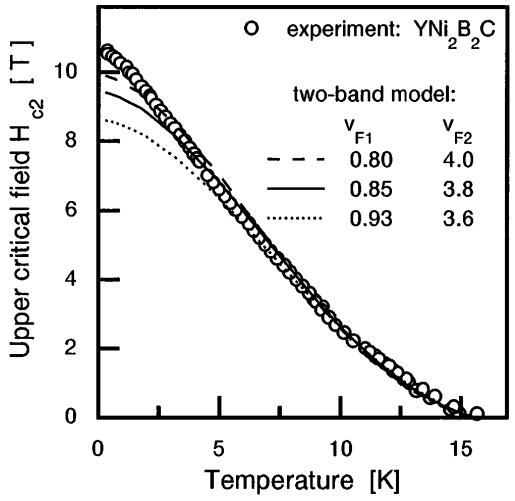

FIG. 2. Temperature dependence of $H_{c2}(T)$ for YNi_2B_2C. Experimental points for the magnetic field $\vec{H}\|$ c axis. The Fermi velocities of the two-band model are given in units of 10^7 cm/s. For the interaction constants, see the text.

The standard ISB model [27] describes *quantitatively* the renormalization of the physical properties of metals due to electron-phonon (el-ph) interaction. The input parameters are the density of states at E_F, $N(0)$, the Fermi velocity v_F, the impurity scattering rate $\gamma_{\rm imp}$, the Coulomb pseudopotential μ^*, and the spectral function $\alpha^2 F(\omega)$ of the el-ph interaction. These quantities can be determined from a few experimental data: the normal state low-T electronic specific heat $\gamma_S T$, the plasma frequency $\omega_{\rm pl}$ inferred from the optical conductivity, $H_{c2}(0)$, T_c and its isotope exponent α, as well as the normal state low-T dc resistivity $\rho(0) \approx \rho(T_c)$ which, similar to T_D, gives a direct measure of the sample purity. We adopt $\mu^* = 0.1$ for the Coulomb pseudopotential and $\hbar\omega_c = 600$ meV for the energy cutoff in Eq. (2). The total el-ph coupling constant $\lambda = 2 \int d\omega \, \alpha^2 F(\omega)/\omega$ can be estimated from the boron isotope effect $\alpha_B \approx 0.2$ [31] and the phonon spectrum [32].

We first consider $LuNi_2B_2C$. To find a lower bound for λ, we accounted for only the high-energy carbon phonons centered at 50 meV and the boron branch at 100 meV. Fitting the experimental α_B and T_c values, we obtained the partial coupling constants $\lambda_{100} = 0.31$, $\lambda_{50} = 0.22$, and $\lambda = \lambda_{100} + \lambda_{50} = 0.53$, where the subscripts denote the corresponding phonon energies in meV. An upper bound of $\lambda = 0.77$ has been found using the Lu phonons centered near 9 meV ($\lambda_9 = 0.34$) and the same B band ($\lambda_{100} = 0.43$) as in the earlier case. In the following, a wide averaged spectrum with $\lambda = 0.65$ ($\lambda_{100} = 0.37$, $\lambda_{50} = 0.12$, $\lambda_9 = 0.16$) will be used which reproduces the experimental values of α_B and T_c. $N(0) = 11.8$ mJ/mol k_B^2 K^2 has been estimated from the experimental value [8] of $\gamma_S = 2\pi^2 \times k_B^2(1 + \lambda)N(0)/3 = 19.5$ mJ/mol K^2. The value of $v_F = 2.76 \times 10^7$ cm/s follows from the experimental value [33] of the plasma frequency $\hbar\omega_{\rm pl} = \sqrt{4\pi e^2 v_F^2 N(0)/3} = 4.0$ eV. The analogous values for YNi_2B_2C are $\lambda = 0.637$, $N(0) = 11.1$ mJ/mol k_B^2 K^2, $v_F = 3 \times 10^7$ cm/s, and $H_{c2}(0) = 2$ T, where the data of Refs. [8] and [34] have been used.

We solved Eqs. (1)–(5) with these parameter sets for two types of spectral densities $\alpha^2F(\omega)$: (i) a wide spectrum and (ii) a single Einstein mode peaked at $\hbar\omega_E = 42.4$ meV chosen to yield the experimental $T_c = 16.5$ K for $LuNi_2B_2C$ using the same value of $\lambda = 0.65$ as in the first case. The results are shown in Fig. 1. Note that, in the intermediate coupling regime under consideration, as expected, $H_{c2}(T)$ is insensitive to details of the shape of $\alpha^2F(\omega)$ [27] and, in the clean-limit case, it is also insensitive to the actual value of the small scattering rates. Comparing the $LuNi_2B_2C$ data with the ISB curves, one clearly realizes strong deviations. In particular, there is a discrepancy of about 3 between experimental and ISB model values of $H_{c2}(0)$. For YNi_2B_2C the discrepancy even reaches a factor of 5. Therefore it makes no sense to discuss any details of the shape of $H_{c2}(T)$, such as the PC, resulting in deviations of the $H_{c2}(T)$ curves of the order 10% to 20%, until the reason for the large failure that accounts for the magnitude of $H_{c2}(0)$ has been elucidated. This serious difficulty was circumvented in previous studies as follows. First, frequently, the quantity $h_{c2}(T) = -H_{c2}(T)/[T_c(dH_{c2}/dT)_{T=T_c}]$, describing the shape of the $H_{c2}(T)$ curve, was considered, but the *absolute* values of $H_{c2}(T)$ were not discussed at all [7]. Second, since, within the ISB model, $H_{c2}(0)$ is a monotonically *increasing* function of the impurity content, in principle, large $H_{c2}(0)$ values might be obtained. To check this approach [9] we calculated the impurity scattering rate $\gamma_{\rm imp}$ which is required to increase $H_{c2}(0)$ up to the $LuNi_2B_2C$ value of 7.6 T. Thus we obtain $\gamma_{\rm imp} \approx 427$ K, which would lead to $\rho(0) \approx 17$ $\mu\Omega$ cm which strongly deviates from the experimental value $\rho(0) \approx 2.5$ $\mu\Omega$ cm. In this context, we note that our data and those of Ref. [35] show dependencies just opposite to those predicted by the ISB model: $H_{c2}(0)$ and T_c *increase* when $\gamma_{\rm imp}$ decreases. Third, a further parameter, the clean limit coherence length, has been introduced in Ref. [35]. However, this results in the overdetermination of the model parameter set, and the consistency of the two values v_F obtained using (i) a clean-limit coherence length and (ii) normal state data has not been checked. Thus the ISB approach fails to explain simultaneously the three values $\gamma_S = 19.5$ mJ/mol K^2, $\hbar\omega_{\rm pl} = 4$ eV, $H_{c2}(0) = 7.6$ T in the clean limit, and the four values γ_S, $\omega_{\rm pl}$, $H_{c2}(0)$, and $\rho = 2.5$ $\mu\Omega$ cm in the dirty limit. In addition, the ISB model is also unable to explain the small gap values $2\Delta_0/k_BT_c < 3.5$ observed in microwave [36], tunneling [10], and dHvA [37] measurements. Furthermore, the PC of $H_{c2}(T)$ near T_c and the extended quasilinear behavior of $H_{c2}(T)$ down to $T \sim 1$ to 2 K cannot be described within the ISB. The ISB model with a *single* v_F contradicts the dHvA data which clearly show the presence of six different sections $F_\alpha, \ldots, F_\eta$ [18,19] with roughly *two* or *three* groups of v_F's.

Turning to our TBM, we solved Eqs. (1)–(5). For the sake of simplicity, the same phonon spectrum as in the ISB case discussed above has been adopted. We achieve an excellent agreement with the $LuNi_2B_2C$ data (see Fig. 1) for $\lambda_1 = 0.51$, $\lambda_2 = \lambda_{21} = 0.2$, $\lambda_{12} = 0.4$, $\mu_1^* = \mu_2^* = 0.1$, $v_{F2} = 3.7 \times 10^7$ cm/s, $v_{F,1} = 0.96 \times 10^7$ cm/s. For YNi_2B_2C, we used the following set: $\lambda_1 = 0.5$, $\lambda_2 = \lambda_{21} = 0.2$, $\lambda_{12} = 0.4$, $\mu_1^* = \mu_2^* = 0.1$, $v_{F2} = 3.8 \times 10^7$ cm/s, $v_{F1} = 0.85 \times 10^7$ cm/s, and $N(0) = 11$ mJ/mol k_B^2 K^2. Reproducing $T_c = 15.6$ K, the adopted values of $N(0)$ agree well with the LDA value [15] of 9.5 mJ/mol k_B^2 K^2. The plasma frequency $\hbar\omega_{\rm pl} = 4.4$ eV is in accord with $\hbar\omega_{\rm pl} = 4.25$ eV obtained in Ref. [34]. From the obtained v_F's it is concluded that $\omega_{\rm pl}$ is related mainly to the second weakly coupled band. Then transport, optical, and tunneling data exhibit mainly the properties of that band, whereas the strongly coupled band remains almost hidden. The calculated value of the penetration depth at 4.2 K, 100 nm, is in agreement with the data of Ref. [35]. Our $\gamma_S = 17.2$ mJ/mol K^2 should be compared with $\gamma_S = 18.2$ mJ/mol K^2 reported in Ref. [8]. Finally, we arrive at $H_{c2}(0) = 9.4$ to 9.9 T, in good agreement with our experimental value $H_{c2}(0) = 10.6 \pm 0.2$ T. The experimental $H_{c2}(T)$ curve of YNi_2B_2C, together with the results of the TBM, are shown in Fig. 2. The values $v_F \approx 4.2 \times 10^7$ cm/s and 0.7 to 1.3×10^7 cm/s of the extremal orbits F_β and $F_{\eta 1/2}$, respectively, derived from earlier dHvA data [18,19] on the same YNi_2B_2C single crystal do not deviate much from the parameters $v_{F2} \approx 3.8 \times 10^7$ cm/s and $v_{F1} \approx 0.8$ to 0.96×10^7 cm/s introduced empirically in our approach. The remaining deviations might be due to natural differences between v_F's on extremal orbits seen in the dHvA experiments and the corresponding *effective* quantities of our TBM which contains implicit information on the whole Fermi surface.

Within our TBM, the PC of $H_{c2}(T)$ depends mainly upon the strength of the interband coupling ($\lambda_{12}, \lambda_{21}$) and to a lesser extent upon the ratio of the Fermi velocities and

the intraband coupling strength (λ_1, λ_2). These findings may also be interpreted in terms of the flat Ni-derived band near E_F and of the dispersive bands crossing E_F seen in the LDA-band structure [14]. The strong mixing of these bands might be viewed as the microscopic origin for significant interband coupling. Further work is required to clarify this point. For $T < 4$ K, $H_{c2}(T)$ is very sensitive to the actual $v_{F,2}/v_{F,1}$ ratio. This is illustrated by the additional curves shown in Fig. 2. The variation of v_{F1} and v_{F2} results in slightly higher and lower $H_{c2}(0)$ values, respectively. Our empirical parameter sets for $LuNi_2B_2C$ and YNi_2B_2C differ almost only in their v_{F1} values which roughly scale with the Ni-Ni distance as $d_{\mathrm{Ni-Ni}}^{-5}$. In this context the study of $Sc(Th)Ni_2B_2C$ having much reduced (increased) Ni-Ni distances is of interest.

Thus, both compounds can be well described within an effective two-band model, provided there are at least two groups of electrons having (i) significantly different Fermi velocities, (ii) strong coupling in the small-v_F band, as well as (iii) sizable coupling between the small-v_F and large-v_F band. This case differs from the situation considered in Refs. [24] and [26]. There, the stronger coupling is in the large-v_F band and the curvature of $H_{c2}(T)$ near T_c is *negative*. A PC would appear only at intermediate T if the interband coupling and the impurity scattering are both weak. In contrast, in this region, $H_{c2}(T)$ shows almost no curvature in our model. In other words, the result of Refs. [24] and [26] can be understood as an average over two weakly coupled superconductors, the first with a high $H_{c2}(0)$ but a low T_c and the second with a small $H_{c2}(0)$ but high T_c. In our case, the isolated small-v_F subsystem would have high values of λ, $H_{c2}(0)$, and T_c. The values of $H_{c2}(0)$ and T_c of the coupled system are reduced by the second large-v_F subsystem with weak interaction parameters. In this case, which to our knowledge has not been considered so far, the PC of the resulting $H_{c2}(T)$ near T_c becomes a direct manifestation of that interband coupling. In our TBM, the PC of $H_{c2}(T)$, as well as $H_{c2}(0)$, and T_c is suppressed by growing impurity content, and the PC vanishes upon reaching the dirty limit with $T_c \approx 11$ K.

In summary, we have shown that the superconductivity of pure nonmagnetic borocarbides should be described within a multiband picture. The isotropic TBM gives a reasonable starting point toward the understanding of the mechanism of superconductivity in these compounds. Combined studies of quantum oscillations (dHvA) and $H_{c2}(T)$ unified by Eliashberg analysis are found to be valuable supplementary tools which are used to elucidate the specific role of subgroups of electrons having small v_F's and strong coupling to bosons. These electrons may be readily overlooked by other experimental techniques.

We thank O. Dolgov, D. Rainer, E. Maksimov, H. Braun, N. Schopohl, and M. Golden for discussions. This work was supported by the INTAS-93-2154 grant, the SFB 463, and the Deutsche Forschungsgemeinschaft.

*On leave from Inst. of Spectros. RAS, Troitsk, Russia.

[1] R. J. Cava *et al.*, Nature (London) **367**, 146 (1994).
[2] R. Nagarajan *et al.*, Phys. Rev. Lett. **72**, 274 (1994).
[3] B. K. Cho *et al.*, Phys. Rev. B **52**, R3844 (1995).
[4] K. Eversmann *et al.*, Physica (Amsterdam) **266C**, 27 (1996).
[5] K.-H. Müller *et al.*, J. Appl. Phys. **81**, 4240 (1997).
[6] C. C. Lai *et al.*, Phys. Rev. B **51**, 420 (1995).
[7] V. Metlushko *et al.*, Phys. Rev. Lett. **79**, 1738 (1997).
[8] H. Michor *et al.*, Phys. Rev. B **52**, 16 165 (1995).
[9] K. D. D. Rathnayaka *et al.*, Phys. Rev. B **55**, 8506 (1997).
[10] Y. De Wilde *et al.*, Phys. Rev. Lett. **78**, 4273 (1997).
[11] S. R. Bahcall, Phys. Rev. Lett. **75**, 1376 (1995).
[12] G. Kotliar *et al.*, Phys. Rev. Lett. **77**, 2296 (1996).
[13] A. S. Alexandrov, Phys. Rev. B **48**, 10 571 (1993).
[14] W. E. Pickett *et al.*, Phys. Rev. Lett. **72**, 3702 (1994).
[15] J. I. Lee *et al.*, Phys. Rev. B **50**, 4030 (1994).
[16] A. A. Abrikosov, Phys. Rev. B **56**, 5112 (1997).
[17] M. Heinecke and K. Winzer, Z. Phys. B **98**, 147 (1995).
[18] G. Goll *et al.*, Phys. Rev. B **53**, R8871 (1996).
[19] L. H. Nguyen *et al.*, J. Low Temp. Phys. **105**, 1653 (1996).
[20] Using the most complete dHvA data available for YNi_2B_2C, only the mean free path $l_q = \hbar v_F/2\pi k_B T_D$ for electrons belonging to different cross sections can be estimated as 181, 86, 56, and 30 nm, where the Fermi velocities v_F of 4.2, 2, 1.3, and 0.7×10^7 cm/s, respectively, and the Dingle temperature $T_D = 2.8$ K have been used. From $\rho(0) \approx \rho_n = 2.5\ \mu\Omega$ cm, $l_\rho = 4\pi v_F/\omega_{\mathrm{pl}}^2 \rho(0)$, only the mean free paths of the large v_F bands can be estimated as $l_\rho \approx 41$ (45) nm, where $\omega_{\mathrm{pl}} = 4.25$ (4.0) eV and $v_F = 3.6$ (3.7) $\times 10^7$ cm/s have been used. All estimated l's exceed significantly the GL coherence length $\xi_0 = \sqrt{\Phi_0/2\pi H_{c2}(0)} = 5.5$ (6.5) nm for YNi_2B_2C ($LuNi_2B_2C$).
[21] Note that the term "two band" should not be taken too literally. Within the Eliashberg theory [23–26], a single anisotropic band model is equivalent to an isotropic multiband model more suitable for theoretical studies.
[22] H. Suhl *et al.*, Phys. Rev. Lett. **3**, 552 (1959).
[23] M. Prohammer *et al.*, Phys. Rev. B **36**, 8353 (1987).
[24] P. Entel *et al.*, J. Low Temp. Phys. **22**, 613 (1976).
[25] P. B. Allen, Phys. Rev. B **13**, 1416 (1976).
[26] E. Langmann, Phys. Rev. B **46**, 9104 (1992).
[27] J. P. Carbotte, Rev. Mod. Phys. **62**, 1027 (1990).
[28] H. Schmidt *et al.*, Physica (Amsterdam) **235C-240C**, 779 (1994).
[29] B. J. Suh *et al.*, Phys. Rev. B **53**, R6022 (1996).
[30] N. R. Werthamer *et al.*, Phys. Rev. **147**, 295 (1966).
[31] D. D. Lawrie *et al.*, Physica (Amsterdam) **245C**, 159 (1995).
[32] F. Gompf *et al.*, Phys. Rev. B **55**, 9058 (1997).
[33] F. Bommeli *et al.*, Phys. Rev. Lett. **78**, 547 (1997).
[34] K. Widder *et al.*, Europhys. Lett. **30**, 55 (1995).
[35] H. Schmidt *et al.*, Phys. Rev. B **55**, 8497 (1997).
[36] T. Jacobs *et al.*, Phys. Rev. B **52**, R7022 (1995).
[37] T. Terashima *et al.*, Phys. Rev. B **56**, 5120 (1997).